

Numerical Heat Transfer, Part B: Fundamentals



ISSN: 1040-7790 (Print) 1521-0626 (Online) Journal homepage: http://www.tandfonline.com/loi/unhb20

IMPROVEMENTS TO INCOMPRESSIBLE FLOW CALCULATION ON A NONSTAGGERED CURVILINEAR GRID

S. Acharya & F. H. Moukalled

To cite this article: S. Acharya & F. H. Moukalled (1989) IMPROVEMENTS TO INCOMPRESSIBLE FLOW CALCULATION ON A NONSTAGGERED CURVILINEAR GRID, Numerical Heat Transfer, Part B: Fundamentals, 15:2, 131-152, DOI: 10.1080/10407798908944897

To link to this article: http://dx.doi.org/10.1080/10407798908944897

	Published online: 27 Apr 2007.
	Submit your article to this journal 🗹
hil	Article views: 48
a a	View related articles 🗗
4	Citing articles: 45 View citing articles 🗹

Full Terms & Conditions of access and use can be found at http://www.tandfonline.com/action/journalInformation?journalCode=unhb20

IMPROVEMENTS TO INCOMPRESSIBLE FLOW CALCULATION ON A NONSTAGGERED CURVILINEAR GRID

S. Acharya and F. H. Moukalled

Mechanical Engineering Department, Louisiana State University, Baton Rouge, Louisiana 70803

The semi-implicit method for pressure-linked equations (SIMPLE) algorithm of Rhie and Chow [6] for flow problems on nonstaggered curvilinear grids is extended, and a SIMPLE-revised (SIMPLER) algorithm is formulated on nonstaggered curvilinear grids. In addition, a new algorithm, SIMPLE-modified (SIMPLEM), is formulated. The performance of these three algorithms is examined through two test problems (driven flow in a cavity and flow in a sudden expansion). The integral form of the continuity equation is shown to be not satisfied in the SIMPLE formulation. In the SIMPLER formulation, the residuals of the momentum equation do not decrease to acceptably low values. The SIMPLEM algorithm shows reasonably good convergence behavior and is superior to both the SIMPLE and SIMPLER algorithms. On the basis of these comparisons, the SIMPLEM algorithm is recommended for use in nonstaggered curvilinear meshes.

INTRODUCTION

In solving incompressible flow equations, a staggered grid (Fig. 1a) is generally used in finite difference methods to eliminate the possibility of predicting checkerboard pressure and velocity fields [1, 2]. Such unrealistic fields are linked to the fact that the first derivative of pressure appears in the momentum equation, but pressure does not have an explicit equation for itself even though its values are implicitly specified by the continuity constraint. When pressure and velocities are stored at the same grid point (nonstaggered grid, Fig. 1b) and when central differences are used to express the firstorder derivatives of pressure in the momentum equation and velocity in the continuity equation, pressure and velocity differences between alternate grid points result in the system of equations. Therefore the momentum equations detect no difference between a uniform and a checkerboard pressure field, whereas the continuity equation is satisfied by both uniform and checkerboard velocity fields. These checkerboard pressure and velocity fields are eliminated if a staggered grid arrangement such as that shown in Fig. la is used. In such a grid system, pressure and velocity differences between adjacent (rather than alternate) grid points are involved in the system of equations, and hence checkerboard pressure and velocity fields are inadmissible.

The primary disadvantage of the staggered grid arrangement is the greater geometrical, and therefore, mathematical complexity associated with three sets of grids (one for the x-component of velocity, one for the y-component of velocity, and one for pressure and other scalar variables). These complexities are particularly overwhelming in curvilinear coordinate systems. It is therefore desirable to calculate the pressure and velocity

NOMENCLATURE				
a, A	coefficients in the discretized equation	ξ	transformed coordinate	
b, B	coefficients of the pressure gradient	ρ	density	
	term in the ξ direction	φ	dependent variable	
c, C	coefficients of the pressure gradient	Γ	diffusion coefficient	
	term in the η direction	Δξ	control volume spacing in ξ-direction	
c_p	specific heat at constant pressure	$\Delta \eta$	control volume spacing in η-direction	
<i>Ġ</i> G	contravariant velocity component contravariant term corresponding to u and v	Subscripts		
J	jacobian	e, n, s, w	east, north, south, and west control	
k k	thermal conductivity		volume faces surrounding grid point F	
L	characteristic length	E, N, S,		
Re	Reynolds number	W	east, north, south, and west grid	
s. S	source terms		points surrounding grid point P	
s, s u. U	x-component of velocity	P	main grid point	
ν, <i>V</i>	y-component of velocity	1	corresponding to the x-momentum	
v, r v, u	temporary velocity variables		equation	
x. X	cartesian coordinate direction	2	corresponding to the y-momentum	
л, л у, <i>Y</i>	cartesian coordinate direction		equation	
•	metric quantity $(x_n^2 + y_n^2)$			
α β		Superscripts		
•	metric quantity $(x_{\xi} + x_{\eta} + y_{\xi}y_{\eta})$ metric quantity $(x_{\xi}^2 + y_{\xi}^2)$	_		
γ እ	central difference operator	·	previous iteration value	
δξ	grid point spacing in \(\xi\)-direction		correction value	
ος δη	grid point spacing in η -direction	1	corresponding to the x-momentum	
•	transformed coordinate		equation	
η μ	viscosity	2	corresponding to the y-momentum equation	

components at the same location but in such a way that unrealistic fields are not predicted. Such methods have been presented by Abdallah [3], Hsu [4], Reggio and Camarero [5], and Rhie and Chow [6]. In [3] the pressure poisson equation is obtained by adding the derivatives of the momentum equations. The momentum equations are solved by an explicit formulation. Unrealistic fields are avoided by ensuring that the boundary conditions exactly satisfy compatibility conditions. In [4], [5], [6], and the present paper, the pressure equation is obtained by combining the continuity and momentum equations as in the semi-implicit method for pressure-linked equations (SIMPLE) method [2] or the SIMPLE-revised (SIMPLER) method [9]. Hsu [4] developed special interpolation expressions from the momentum equations for the mass fluxes leaving the faces of a control volume surrounding a grid point. These expressions, which contain pressure differences between adjacent nodes, are used in the continuity equation to obtain the equation for pressure, and a SIMPLER type algorithm is used in the calculations. Reggio and Camarero [5] used an overlapping nonstaggered grid with forward and backward differencing for mass and pressure gradients, respectively, and the SIMPLE algorithm was used in the calculations. Rhie and Chow [6] added a correction term to the mass fluxes along the control volume faces. This correction term is proportional to the difference between a pressure gradient calculated by a centered $2-\delta$ ($2\delta-\xi$ or $2\delta-\eta$) difference scheme and a pressure gradient calculated on a 1- δ difference scheme. Thus the correc-

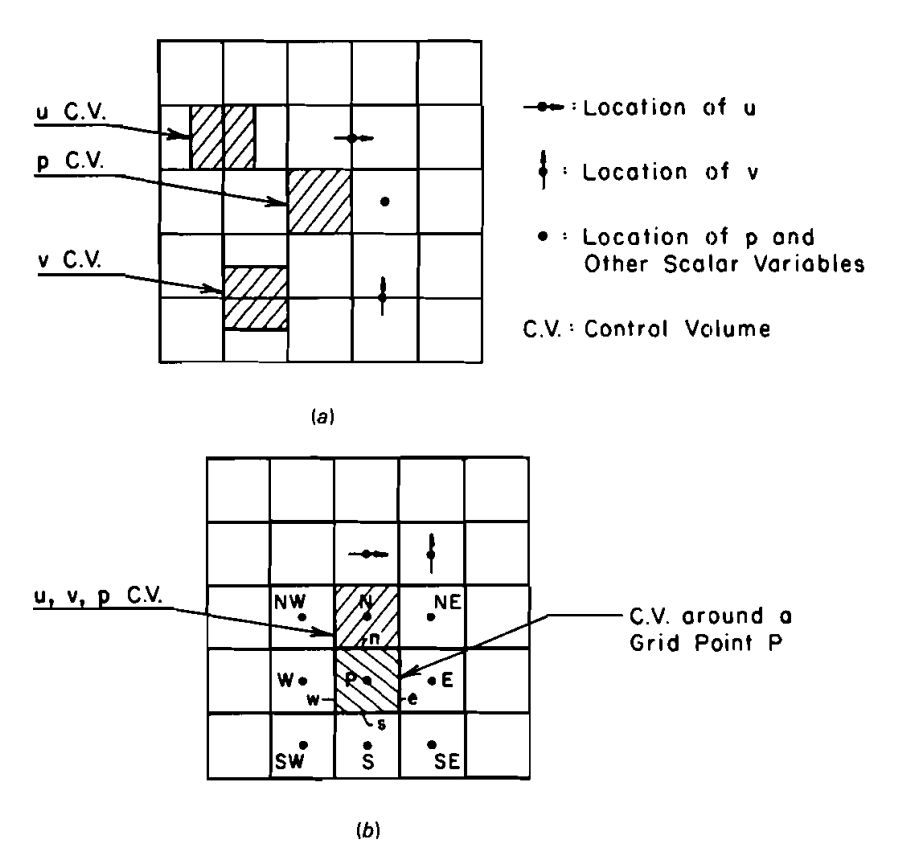


Fig. 1 (a) Staggered grid arrangement for two-dimensional situations. (b) Nonstaggered grid arrangement for two-dimensional situations.

tion term immediately detects and suppresses the development of checkerboard pressure fields. Only the SIMPLE algorithm was used in their calculations, and the method was applied to flow over an airfoil. No results were presented, however, regarding the convergence characteristics of the momentum and continuity equations or the degree to which conservation was satisfied.

Similar efforts in equally representing the pressure and velocity fields (called equal-order interpolation) have been undertaken in the finite element literature. Examples of such efforts have been reported by Schneider, Raithby, and Yovanovich [7] and by Sani et al. [8].

This paper has two objectives. The first is to extend the method of Rhie and Chow [6] (which used the SIMPLE algorithm) to the SIMPLER algorithm and to evaluate the convergence characteristics of the two methods and the degree to which conservation over each control volume is satisfied. The second is to present a new algorithm, SIMPLE-modified (SIMPLEM), which is shown to be considerably superior to the SIMPLE and SIMPLER algorithms on nonstaggered curvilinear grids. The unique features of this algorithm are its simplicity, its good convergence characteristics, and its ability to suppress checkerboard pressure and velocity fields.

GOVERNING EQUATIONS

In cartesian coordinates, the momentum and mass conservation equations can be written as

$$\frac{\partial}{\partial x}(\rho u\phi) + \frac{\partial}{\partial y}(\rho v\phi) = \frac{\partial}{\partial x}\left(\Gamma\frac{\partial\phi}{\partial x}\right) + \frac{\partial}{\partial y}\left(\Gamma\frac{\partial\phi}{\partial y}\right) + S \tag{1}$$

where ϕ is 1 for the mass conservation equation, u for the conservation of x-momentum, and v for the conservation of y-momentum. The diffusion coefficient is denoted by Γ , and S is the source term. If curvilinear coordinates ξ and η are introduced, Eq. (1) can be transformed according to the general transformation $\xi = \xi(x, y)$ and $\eta = (x, y)$ and can be rewritten as

$$\frac{\partial}{\partial \xi} \left[\rho G_1 \phi - \left(\frac{\Gamma}{J} \right) \left(\alpha \frac{\partial \phi}{\partial \xi} - \beta \frac{\partial \phi}{\partial \eta} \right) \right]$$

$$+ \frac{\partial}{\partial \eta} \left[\rho G_2 \phi - \left(\frac{\Gamma}{J} \right) \left(\gamma \frac{\partial \phi}{\partial \eta} - \beta \frac{\partial \phi}{\partial \xi} \right) \right] = SJ$$
 (2)

where α , β , γ , and the jacobian J are given by

$$\alpha = \left(\frac{\partial x}{\partial \eta}\right)^2 + \left(\frac{\partial y}{\partial \eta}\right)^2 \tag{3}$$

$$\beta = \frac{\partial x}{\partial \xi} \frac{\partial x}{\partial \eta} + \frac{\partial y}{\partial \xi} \frac{\partial y}{\partial \eta} \tag{4}$$

$$\gamma = \left(\frac{\partial x}{\partial \xi}\right)^2 + \left(\frac{\partial y}{\partial \xi}\right)^2 \tag{5}$$

$$J = \frac{\partial x}{\partial \xi} \frac{\partial y}{\partial n} - \frac{\partial x}{\partial n} \frac{\partial y}{\partial \xi} \tag{6}$$

and the contravariant velocity components G_1 and G_2 are defined as

$$G_1 = u \frac{\partial y}{\partial \eta} - v \frac{\partial x}{\partial \eta} \tag{7}$$

$$G_2 = v \frac{\partial x}{\partial \xi} - u \frac{\partial y}{\partial \xi} \tag{8}$$

The differential terms in parentheses on the left side of Eq. (2) represent the total fluxes across lines of constant ξ and η , respectively.

In obtaining the discrete approximation of Eq. (2) on a nonstaggered curvilinear grid, the governing differential equation is integrated over the control volume surround-

ing a grid point P (see Fig. 1b for example), and profile approximations are made in each coordinate direction. This results in the following system of equations. X-momentum:

$$a_P^1 u_P = \sum_{n \in \text{EWNS}} a_n^1 u_n + s_1 + \left(b_1 \frac{\partial p}{\partial \xi} + c_1 \frac{\partial p}{\partial \eta} \right)_P \tag{9}$$

Y-momentum:

$$a_P^2 v_P = \sum_{n=E,W,N,S} a_n^2 v_n + s_2 + \left(b_2 \frac{\partial p}{\partial \xi} + c_2 \frac{\partial p}{\partial \eta} \right)_P$$
 (10)

Continuity:

$$(\rho G_1 \Delta \eta)_{\sigma} - (\rho G_1 \Delta \eta)_{w} + (\rho G_2 \Delta \xi)_{n} - (\rho G_2 \Delta \xi)_{s} = 0 \tag{11}$$

where u_p denotes the velocity at the point P; u_n denotes the velocity at its four neighbors, E, W, N, and S; and a_p^1 and a_n^1 are the corresponding coefficients whose expressions depend on the nature of the profile approximations made. In the present work the power-law profile approximation recommended by Patankar [9] is chosen. The term s_1 is the x-momentum source term, and b_1 and c_1 are given by the following expressions:

$$b_1 = -\left(\frac{\partial y}{\partial \eta}\right) \Delta \xi \ \Delta \eta \qquad c_1 = \left(\frac{\partial y}{\partial \xi}\right) \Delta \xi \ \Delta \eta \tag{12}$$

A similar nomenclature applies to the y-momentum equation [Eq. (10)]. Equations (9) and (10) can be re-expressed simply as

$$u_{P} = \sum_{n=E,W,N,S} A_{n}^{1} u_{n} + S_{1} + \left(B_{1} \frac{\partial p}{\partial \xi} + C_{1} \frac{\partial p}{\partial \eta} \right)_{P}$$
 (13)

$$v_P = \sum_{n=E,W,S,S} A_n^2 v_n + S_2 + \left(B_2 \frac{\partial p}{\partial \xi} + C_2 \frac{\partial p}{\partial \eta} \right)_P$$
 (14)

where

$$A_n^1 = \frac{a_n^1}{a_n^1}$$
 $S_1 = \frac{s_1}{a_n^1}$ $B_1 = \frac{b_1}{a_n^1}$ $C_1 = \frac{c_1}{a_n^1}$ (15)

and

$$A_n^2 = \frac{a_n^2}{a_P^2}$$
 $S_2 = \frac{S_2}{a_P^2}$ $B_2 = \frac{b_2}{a_P^2}$ $C_2 = \frac{c_2}{a_P^2}$ (16)

SIMPLE AND SIMPLER ALGORITHMS ON NONSTAGGERED CURVILINEAR GRIDS

SIMPLE Algorithm

The pressure-correction equation is used in the SIMPLE algorithm to update both velocity and pressure. The pressure correction p' is a correction to the currently available estimate for pressure (p^*) , so that the correct pressure field $p = p^* + p'$ when substituted into the momentum equation produces a continuity-satisfying velocity field. If u^* is the velocity field based on p^* , then Eq. (13) can be written as

$$u_{P}^{*} = \sum_{n=\text{E.W.N.S}} A_{n}^{1} u_{n}^{*} + S_{1} + \left(B_{1} \frac{\partial p^{*}}{\partial \xi} + C_{1} \frac{\partial p^{*}}{\partial \eta} \right)_{P}$$
 (17)

Subtracting Eq. (17) from Eq. (13) and arbitrarily dropping the $\sum A_n^1(u_n - u_n^*)$ term results in the velocity-correction equation

$$u_p = u_p^* + \left(B_1 \frac{\partial p'}{\partial \xi} + C_1 \frac{\partial p'}{\partial \eta}\right)_P \tag{18}$$

A similar equation can be written for v_n :

$$v_P = v_P^* + \left(B_2 \frac{\partial p'}{\partial \xi} + C_2 \frac{\partial p'}{\partial \eta} \right)_P \tag{19}$$

The corresponding correction equations for G_1 and G_2 can be obtained by substituting Eqs. (18) and (19) into Eqs. (7) and (8). This results in

$$G_1 = G_1^* + \left(B_1 \frac{\partial y}{\partial \eta} - B_2 \frac{\partial x}{\partial \eta}\right) \frac{\partial p'}{\partial \xi} + \left(C_1 \frac{\partial y}{\partial \eta} - C_2 \frac{\partial x}{\partial \eta}\right) \frac{\partial p'}{\partial \eta}$$
(20)

and

$$G_2 = G_2^* + \left(C_2 \frac{\partial x}{\partial \xi} - C_1 \frac{\partial y}{\partial \xi}\right) \frac{\partial p'}{\partial \eta} + \left(B_2 \frac{\partial x}{\partial \xi} - B_1 \frac{\partial y}{\partial \xi}\right) \frac{\partial p'}{\partial \xi}$$
(21)

If the grid is orthogonal, the last terms in Eqs. (20) and (21) are negligible. Neglecting these terms, G_1 and G_2 can be written as

$$G_1 = G_1^* + B \frac{\partial p'}{\partial \xi} \tag{22}$$

$$G_2 = G_2^* + C \frac{\partial p'}{\partial \eta} \tag{23}$$

where

$$B = B_1 \frac{\partial y}{\partial \eta} - B_2 \frac{\partial x}{\partial \eta} \qquad C = C_2 \frac{\partial x}{\partial \xi} - C_1 \frac{\partial y}{\partial \xi}$$
 (24)

These approximate relations for G_1 and G_2 [Eqs. (22) and (23)] can be used to derive new correction equations for u and v as follows:

$$u = u^* + \left[\left(\frac{\partial x}{\partial \xi} \right) B \left(\frac{\partial p'}{\partial \xi} \right) + \left(\frac{\partial x}{\partial \eta} \right) C \left(\frac{\partial p'}{\partial \eta} \right) \right] / J \tag{25}$$

$$v = v^* + \left[\left(\frac{\partial y}{\partial \xi} \right) B \left(\frac{\partial p'}{\partial \xi} \right) + \left(\frac{\partial y}{\partial \eta} \right) C \left(\frac{\partial p'}{\partial \eta} \right) \right] / J \tag{26}$$

The pressure-correction equation is obtained by substituting G_1 and G_2 from Eqs. (22) and (23) into the continuity equation [Eq. (11)]. Its final form is given by

$$a_P p_P' = \sum_{n=E,W,N,S} a_n p_n' + b$$
 (27)

where

$$a_{\rm E} = -(\rho B)_{\rm e} \left(\frac{\Delta \eta}{\delta \xi}\right)_{\rm e} \tag{28}$$

$$a_{\rm W} = -(\rho B)_{\rm w} \left(\frac{\Delta \eta}{\delta \xi}\right)_{\rm w} \tag{29}$$

$$a_{\rm N} = -(\rho C)_{\rm n} \left(\frac{\Delta \xi}{\delta \eta}\right)_{\rm n} \tag{30}$$

$$a_{\rm S} = -(\rho C)_{\rm s} \left(\frac{\Delta \xi}{\delta \eta}\right)_{\rm s} \tag{31}$$

$$a_P = a_E + a_W + a_N + a_S (32)$$

$$b = (\rho G_1^* \Delta \eta)_w - (\rho G_1^* \Delta \eta)_e + (\rho G_2^* \Delta \xi)_s - (\rho G_2^* \Delta \xi)_n$$
 (33)

In Eq. (33), b is the local imbalance of mass and the subscripts e, w, n, and s refer to the interfaces of a control volume (see Fig. 1). In the SIMPLE algorithm, once the pressure-correction field is obtained, pressure is updated by adding p' to p^* and velocities are updated by using Eqs. (25) and (26). When updating u and v, a second-order centered $2-\delta$ ($2\delta-\xi$ or $2\delta-\eta$) difference scheme is used for the pressure-correction gradients at the grid nodes. The contravariant components G_1 and G_2 are needed at the interfaces and are updated by using a $1-\delta$ difference scheme for the pressure-correction gradients at the control volume faces. Oscillations in the pressure field are thus detected by G_1 and G_2 , which are always used in the momentum equations. This practice alone is

however, insufficient to suppress spurious oscillations completely. This is because, after the momentum equations are solved to obtain u and v, the contravariant velocities G_1 and G_2 are calculated at the nodes by using Eqs. (7) and (8) and linear interpolation is used to calculate the interface values. These interface contravariant values (G_1 and G_2) are used in calculating the source term of the p' equation, but because they are obtained by linear interpolation and because a $2\delta - \xi$ (or $2\delta - \eta$) scheme for ∇p is used in the momentum equation, spurious oscillations may not be easily destroyed. In view of this, Rhie and Chow [6] added the following correction term to G^* in the source term of the pressure-correction equation to eliminate oscillations in the predicted solutions.

$$(G_{i}^{*})_{c} = \hat{G}_{i}^{*} + \bar{B} \left[\frac{(p_{E} - p_{P})}{\delta \xi} - \left(\frac{\overline{\partial p}}{\overline{\partial \xi}} \right) \right]$$
(34)

where the overbar indicates that the results are obtained by linear interpolation between grid nodes. This practice, although successful in suppressing oscillations, suffers from the problem of satisfying continuity and is discussed later.

The SIMPLE algorithm consists of the following steps.

- 1. Start with guessed fields u^* , v^* , and p^* .
- 2. Calculate the coefficients of the momentum equations using a $2\delta \xi$ or $2\delta \eta$ scheme for ∇p , and solve the momentum equations to obtain a new velocity field.
- 3. Calculate new G_1 and G_2 values at the grid nodes using the new values of the velocity components. Interpolate to find G_1 and G_2 at the control volume faces.
- 4. Calculate the correction terms to be added to G_1 and G_2 in the pressure-correction equation (continuity equation) only.
- 5. Calculate the coefficients of the pressure-correction equation, and solve to obtain the pressure-correction field.
- 6. Use the pressure-correction field to update p, u, v, G_1 , and G_2 . The contravariant velocities G_1 and G_2 are updated directly at the control volume faces by using a centered 1- δ difference scheme.
- 7. Return to step 2 and repeat until a converged solution is obtained.

SIMPLER Algorithm

In this paper, a SIMPLER algorithm is developed for nonstaggered curvilinear grids. The rationale for developing this algorithm is based on the demonstrated superiority of the SIMPLER algorithm over the SIMPLE algorithm on staggered grids. A similar superiority is therefore expected on nonstaggered grids.

In SIMPLER, pressure is updated through an equation for pressure and velocity is updated through the pressure-correction equation. The pressure equation is derived by writing the momentum equations in the following form:

$$u = u + B_1 \frac{\partial p}{\partial \xi} + C_1 \frac{\partial p}{\partial \eta}$$
 (35)

$$v = v + B_2 \frac{\partial p}{\partial \xi} + C_2 \frac{\partial p}{\partial \eta}$$
 (36)

where

$$u = \sum_{n=E,W,N,S} A_n^1 u_n + S_1$$
 (37)

$$v = \sum_{n=E,W,N,S} A_n^2 v_n + S_2$$
 (38)

With the above definitions of u and v, expressions are obtained for G_1 and G_2 as follows:

$$G_1 = G_1 + \left(B_1 \frac{\partial y}{\partial \eta} - B_2 \frac{\partial x}{\partial \eta}\right) \left(\frac{\partial p}{\partial \xi}\right) + \left(C_1 \frac{\partial y}{\partial \eta} - C_2 \frac{\partial x}{\partial \eta}\right) \left(\frac{\partial p}{\partial \eta}\right)$$
(39)

$$G_2 = G_2 + \left(C_2 \frac{\partial x}{\partial \xi} - C_1 \frac{\partial y}{\partial \xi}\right) \left(\frac{\partial p}{\partial n}\right) + \left(B_2 \frac{\partial x}{\partial \xi} - B_1 \frac{\partial y}{\partial \xi}\right) \left(\frac{\partial p}{\partial \xi}\right)$$
(40)

where

$$G_1 = u \frac{\partial y}{\partial \eta} - v \frac{\partial x}{\partial \eta} \tag{41}$$

$$G_2 = v \frac{\partial x}{\partial \xi} - u \frac{\partial y}{\partial \xi} \tag{42}$$

Introducing these values of G_1 and G_2 into the continuity equation, the final form of the pressure equation is obtained as

$$a_P p_P = \sum_{n=E,W,N,S} a_n p_n + b \tag{43}$$

where $a_{\rm E}$, $a_{\rm W}$, $a_{\rm N}$, $a_{\rm S}$, and $a_{\rm P}$ are given by Eqs. (28) through (32) and

$$b = (\rho G_1 \Delta \eta)_w - (\rho G_1 \Delta \eta)_c + (\rho G_2 \Delta \xi)_s - (\rho G_2 \Delta \xi)_n + b_{\infty}$$
(44)

In Eq. (44), $b_{\rm no}$ is the contribution due to nonorthogonality. It is expressed as

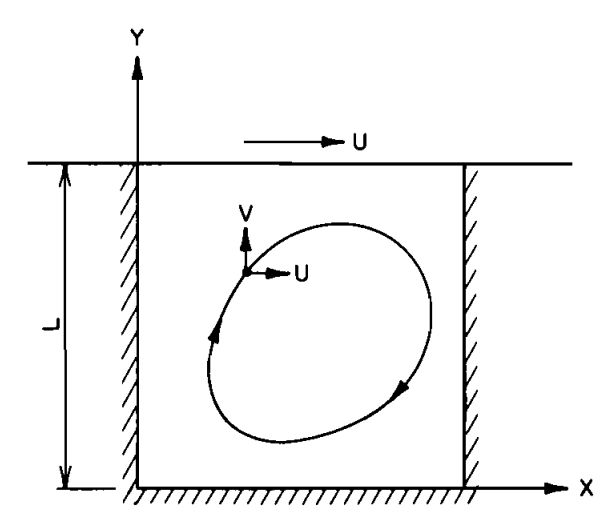


Fig. 2 Recirculating flow in a square cavity.

$$b_{no} = \left[\left(C_1 \frac{\partial y}{\partial \eta} - C_2 \frac{\partial x}{\partial \eta} \right) \left(\frac{\partial p}{\partial \eta} \right) \right]_{w} - \left[\left(C_1 \frac{\partial y}{\partial \eta} - C_2 \frac{\partial x}{\partial \eta} \right) \left(\frac{\partial p}{\partial \eta} \right) \right]_{e} + \left[\left(B_2 \frac{\partial x}{\partial \xi} - B_1 \frac{\partial y}{\partial \xi} \right) \left(\frac{\partial p}{\partial \xi} \right) \right]_{s} - \left[\left(B_2 \frac{\partial x}{\partial \xi} - B_1 \frac{\partial y}{\partial \xi} \right) \left(\frac{\partial p}{\partial \xi} \right) \right]_{n} (45)$$

To avoid checkerboard fields, a correction term as in Eq. (34) is added to the interface contravariant components appearing in the source term of the pressure-correction equation. The specific steps in the SIMPLER algorithm are as follows.

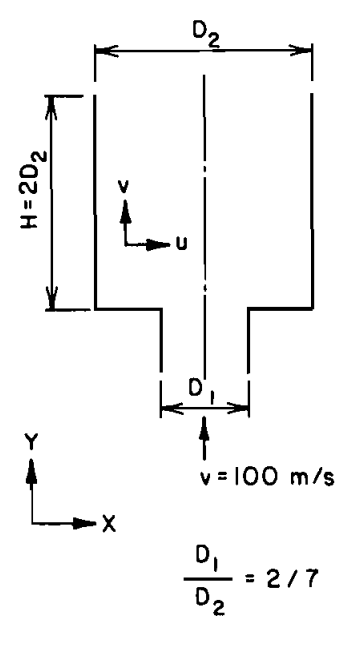


Fig. 3 Recirculating flow due to sudden expansion in a pipe.

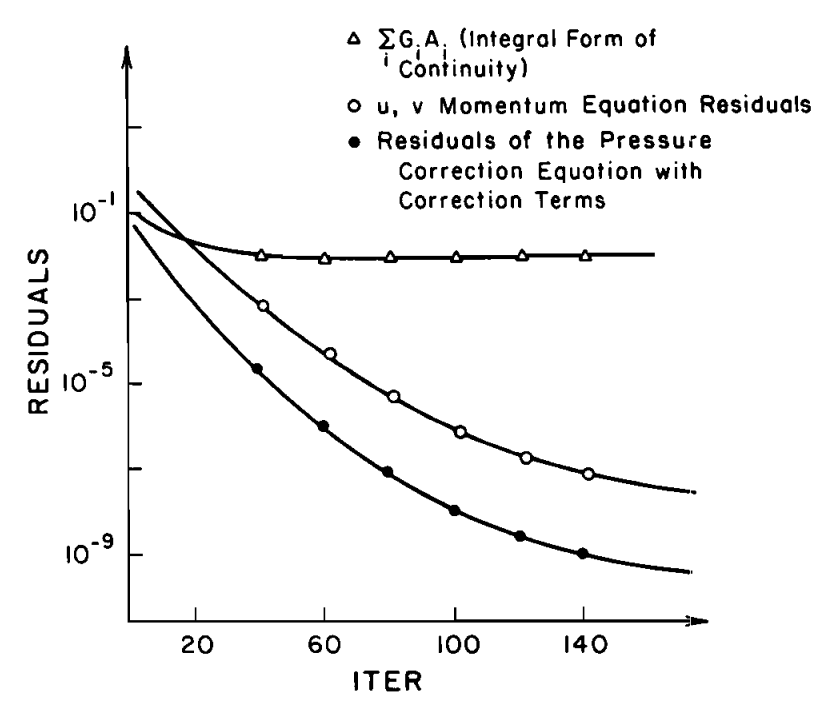


Fig. 4 Maximum residuals of conservation equations for flow in a square cavity on a 15×15 orthogonal mesh obtained with SIMPLE (Re - 100). ITER along the horizontal axis denotes number of iterations.

- 1. Start with guessed fields u^* and v^* .
- 2. Calculate the coefficients of the momentum equations and then u and v. Use these values to find G_1 and G_2 at the grid nodes. Interpolate linearly to find G_1 and G_2 at the control volume faces.
- 3. Calculate the coefficients of the pressure equation, and solve the pressure equation to obtain a new pressure field.
- 4. Use this new pressure field to calculate the pressure gradients in the momentum equations using a $2\delta \xi$ or $2\delta \eta$ centered difference scheme.
- 5. Solve the momentum equations to obtain a new velocity field.
- 6. Use this field to obtain new G_1 and G_2 values at the grid nodes. By linear interpolation, obtain G_1 and G_2 at the control volume faces.
- 7. Calculate the correction terms that will be added to G_1 and G_2 in the source term of the pressure-correction equation.
- 8. Solve the pressure-correction equation to obtain a pressure-correction field.
- 9. Use this field to update u, v, G_1 , and G_2 . Do not update the pressure. Update G_1 and G_2 directly at the interfaces using a 1δ - ξ or 1δ - η centered difference scheme for $\nabla p'$.
- 10. Return to step 2 and repeat until convergence is obtained.

PROPOSED SIMPLEM ALGORITHM ON NONSTAGGERED CURVILINEAR GRIDS

The SIMPLEM algorithm was developed because of the unsatisfactory performances by the SIMPLE and the SIMPLER algorithms and is based on experience gathered from test problems run with these algorithms. In the SIMPLEM algorithm, a pressure equation is used to update the pressure field and also the velocity field such that they satisfy continuity in each step.

The SIMPLEM algorithm consists of the following steps.

- 1. Start with guessed fields u^* and v^* .
- 2. Calculate the coefficients of the momentum equations and then solve for u and v. Use these values to find G_1 and G_2 at the grid nodes. Interpolate linearly to find G_1 and G_2 at the control volume faces.
- 3. Calculate the coefficients of the pressure equation, and solve it to obtain a new pressure field.
- 4. Use this new pressure field to calculate the pressure gradients in the momentum equation using a $2\delta \xi$ or $2\delta \eta$ centered difference scheme.
- 5. Update G_1 and G_2 [Eqs. (39) and (40)] at the interfaces using the new pressure field and a $1\delta \xi$ or $1\delta \eta$ centered difference scheme for ∇p .
- 6. On the basis of the new G_1 and G_2 values, recalculate the coefficients and solve the momentum equations to obtain a new velocity field (u and v values).

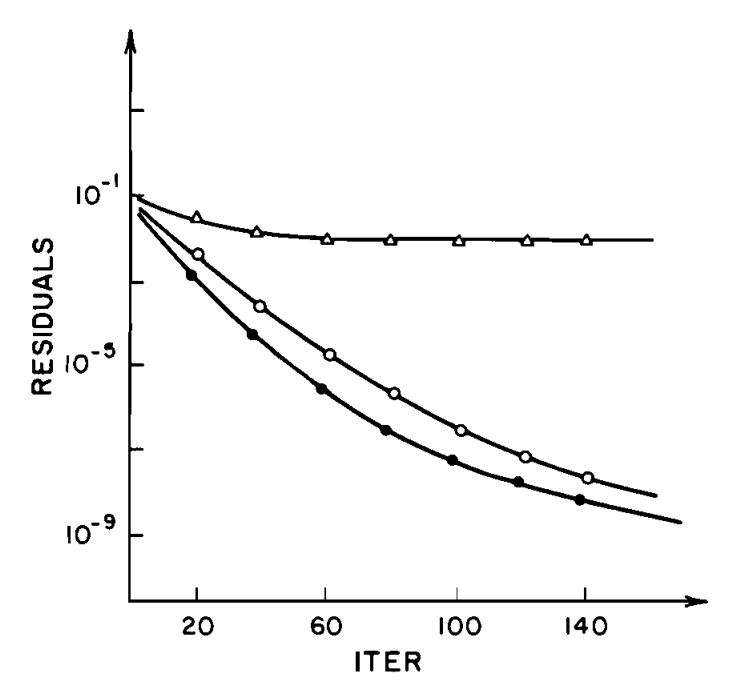


Fig. 5 Maximum residuals of conservation equations for flow in a square cavity on a 15×15 nonorthogonal mesh obtained with SIMPLE (Re - 100). See Fig. 4 for explanation of symbols.

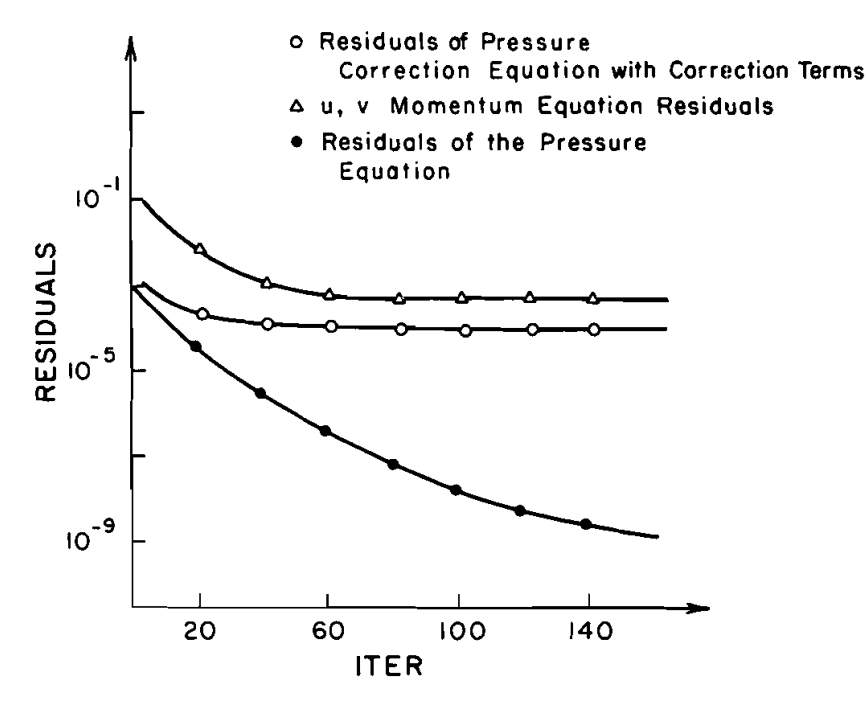


Fig. 6 Maximum residuals of conservation equations for flow in a square cavity on a 15×15 orthogonal mesh obtained with SIMPLER (Re - 100).

7. Use these u and v values as a new guess. Return to step 2 and repeat until a converged solution is obtained.

TEST PROBLEMS AND RESULTS

The three algorithms were used to solve two test problems to determine the convergence characteristics and the degree to which conservation is satisfied.

The first problem, driven flow in a square cavity (Fig. 2), is one of the standard problems used in the literature [4, 10, 11] to test the solution methodology for fluid-flow problems.

By introducing the following dimensionless variables

$$X = \frac{x}{L} \qquad Y = \frac{y}{L} \qquad U = \frac{u}{u_s} \qquad V = \frac{v}{u_s} \qquad P = \frac{p}{\rho u_s^2} \tag{46}$$

where u_s is the velocity of the moving boundary and L is the length of the square cavity, the governing equations for this problem can be written as

$$\nabla \cdot \mathbf{U} = 0 \tag{47}$$

$$\mathbf{U} \cdot \nabla U = -\frac{\partial P}{\partial X} + \frac{\nabla^2 U}{\mathrm{Re}}$$
 (48)

$$\mathbf{U} \cdot \nabla V = -\frac{\partial P}{\partial Y} + \frac{\nabla^2 V}{\text{Re}} \tag{49}$$

The Reynolds number, defined by $\rho u_s L/\mu$, is the only variable parameter in this problem. The results presented are for Reynolds number of 100. The boundary conditions for this problem are zero velocities along all boundaries except at the moving wall, where U is set to 1.

The second problem is sudden expansion in a pipe (Fig. 3). This problem is chosen because of the strong pressure gradients in the domain that can give rise to spurious oscillations if the solution scheme is not appropriately formulated. The governing equations for this problem can be written as

$$\nabla \cdot (\rho \mathbf{u}) = 0 \tag{50}$$

$$\rho \mathbf{u} \cdot \nabla u = \frac{-\partial p}{\partial x} + \mu \nabla^2 u \tag{51}$$

$$\rho \mathbf{u} \cdot \nabla v = \frac{-\partial p}{\partial y} + \mu \nabla^2 v \tag{52}$$

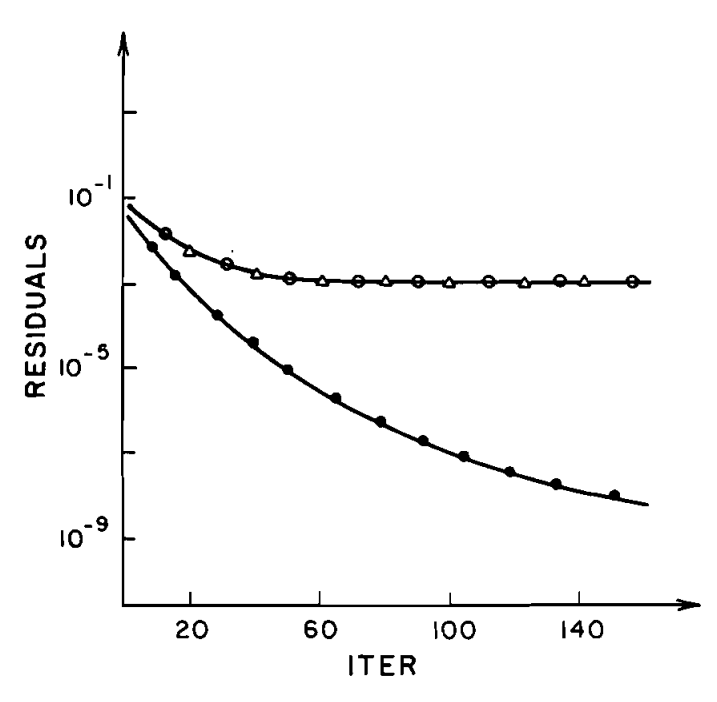


Fig. 7 Maximum residuals of conservation equations for flow in a square cavity on a 15×15 nonorthogonal mesh obtained with SIMPLER (Re - 100). See Fig. 6 for explanation of symbols.

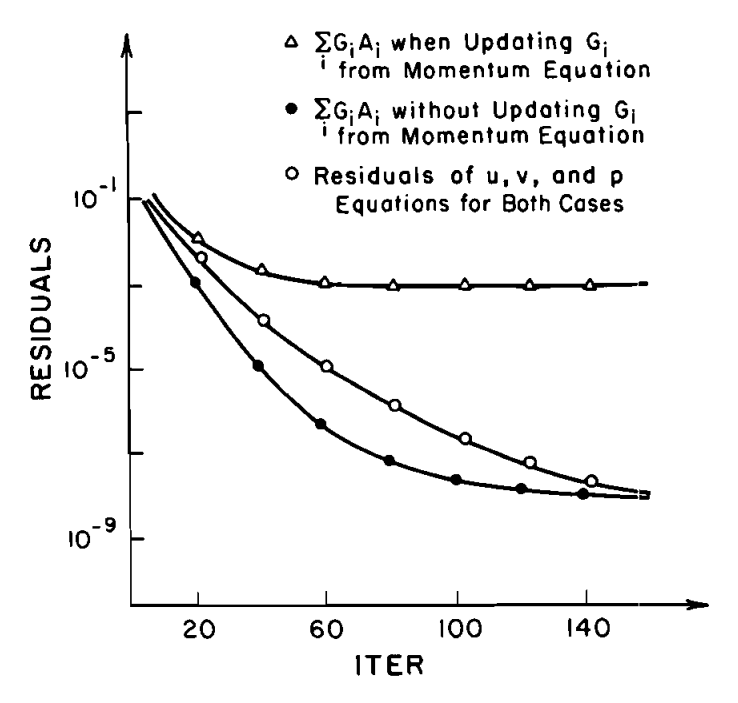


Fig. 8 Maximum residuals of conservation equations for flow in a square cavity on a 15×15 orthogonal mesh obtained with SIMPLEM (Re - 100).

$$\rho \mathbf{i} \cdot \nabla T = \left(\frac{k}{c_p}\right) \nabla^2 T \tag{53}$$

where μ is the viscosity of the fluid used, k is the thermal conductivity, and c_p is the specific heat. At the inlet, a uniform ν -velocity of 100 m/s at room temperature is assumed. Air is taken to be the working fluid, and μ , k, c_p , and ρ for constant density flows are evaluated at the inlet room temperature. Results are also obtained for variable density flows, for which the equation of state is used to calculate the density. Along the outflow boundary a high-Peclet number unidirectional flow is assumed, and the outflow velocity is modified to satisfy overall continuity.

The first problem is solved for both orthogonal and nonorthogonal coordinates. The solution for the second problem is obtained only on an orthogonal grid.

Of primary interest are the maximum residuals of the equations solved and the convergence rate of these residuals. The maximum residual is a commonly used norm to check the convergence rate of a numeric scheme and is adopted here in preference to other alternative norms, such as the root-mean-square value of the residuals or the sum of the magnitude of the residuals.

In Figs. 4, 5, and 10 the maximum residuals of the momentum, continuity [Eq. (11)], and pressure-correction equations [Eq. (27)] obtained by using SIMPLE are presented. All results predict the same behavior. The residuals of the momentum equations and the pressure-correction equation (including the correction terms) are driven to zero.

The residuals of the continuity equation reach a certain level of convergence, however, and stop decreasing further with iterations.

The residuals of the momentum, pressure, and pressure-correction equations when using SIMPLER are presented in Figs. 6, 7, and 11. From these figures, it is clear that all residuals, with the exception of the residuals of the pressure equation, stabilize after reaching a certain level of convergence.

Figures 8, 9, 12, and 13 show the residuals of the various quantities obtained by using the new algorithm SIMPLEM. In all figures, the maximum residuals of u, v, p, and Eq. (11) (the continuity equation) are presented by means of two different practices. The first practice is to update the contravariant velocity components needed at the interfaces after solving the momentum equation (i.e., after step 6 in the SIMPLEM algorithm). In the second practice, outlined earlier, these components are not updated from momentum and therefore are always based on the solution of the pressure equation. All results show the same trend, with maximum conservation obtained for the case when the flow is incompressible and the grid is orthogonal. The residuals of Eq. (11) are computed to study the effect of interpolation on continuity. Furthermore, Eq. (11) is the integral form of the continuity equation, whereas the pressure equation represents the discretized form of continuity.

The residuals of the pressure and momentum equations are always driven to zero. For some of the cases, however, the maximum imbalance of mass [Eq. (11)] converges to a certain extent and stops decreasing further after a number of iterations. This behavior is noticed in a skewed grid or in variable-density flow as shown in Figs. 9 and 12,

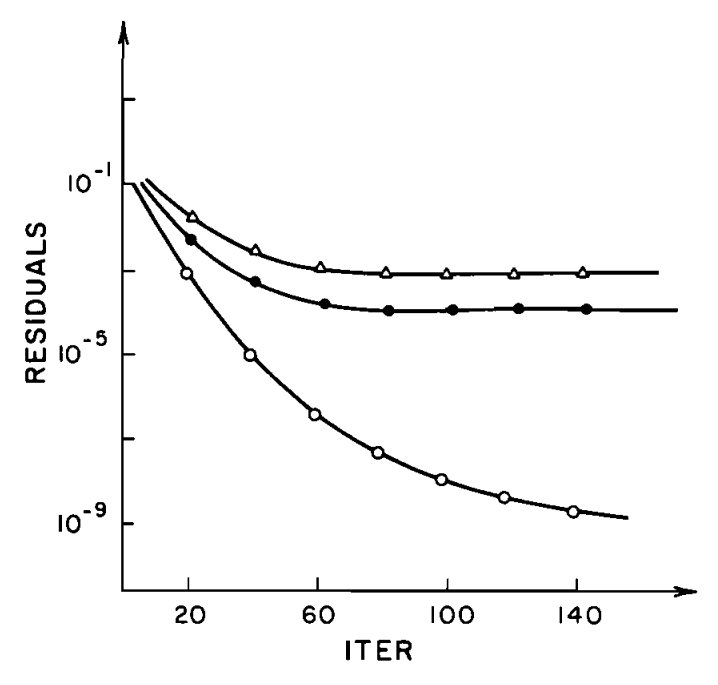


Fig. 9 Maximum residuals of conservation equations for flow in a square cavity on a 15×15 nonorthogonal mesh obtained with SIMPLEM (Re = 100). See Fig. 8 for explanation of symbols.

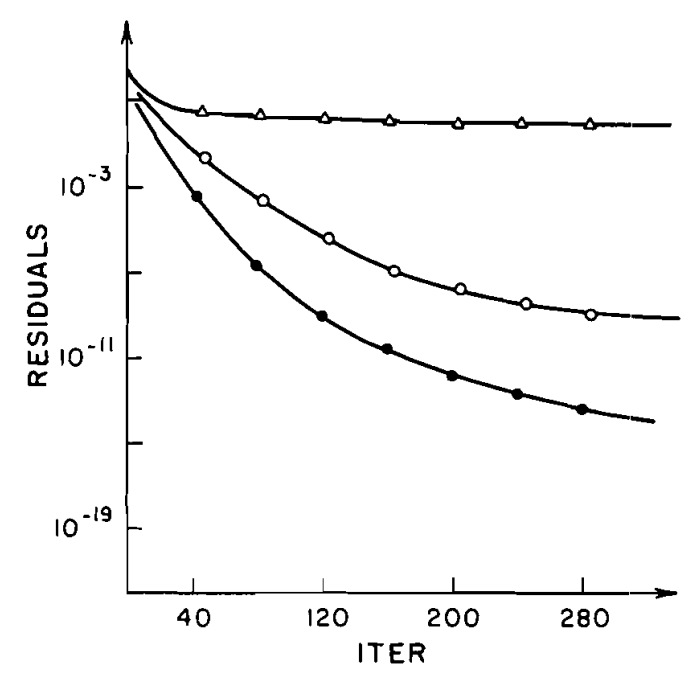


Fig. 10 Maximum residuals of conservation equations for recirculating flow in a sudden expansion obtained with a 14×14 orthogonal mesh and SIMPLE (variable density flow). See Fig. 4 for explanation of symbols.

respectively. In all figures, the practice of updating the contravariant velocity components after solving the momentum equations slows convergence considerably.

DISCUSSION OF RESULTS

In SIMPLE, the integral form of the continuity equation [Eq. (11)] was not satisfied (Figs. 4, 5, and 10). This is attributed to the correction terms added to the interface contravariant velocities appearing in the source term of the pressure-correction equation. These approximations are introduced after, not before, deriving the pressure-correction equation. Therefore the source term b in the pressure-correction equation [Eq. (33)], which represents the local deviation from continuity, is altered by the inclusion of the correction terms and hence is no longer exactly equal to the local mass conservation imbalance. As a result, the pressure-correction equation that is solved is not the discretized continuity equation but rather an approximate form of the continuity equation, with the approximation being of the order of the correction term (which, in some cases, is quite large). This conclusion is confirmed by obtaining results, when possible (i.e., when checkerboard pressure fields can be avoided), for the same problems without adding these correction terms, in which case the residuals of the continuity and pressurecorrection equations are identical and both converge to zero. It is possible to obtain oscillation-free results for the driven cavity flow problem only. Oscillation occurred in the sudden expansion problem, where pressure gradients play a dominant role. Therefore, the addition of these terms is necessary to suppress oscillation effectively. Because

pressure and velocity components are updated from the same pressure-correction equation, convergence of their equations is expected. The results in Figs. 4, 5, and 10 confirm this expectation.

In SIMPLER, a different behavior is noted. Results obtained with the correction terms added to the contravariant velocities in the source term of the pressure-correction equation (Figs. 6, 7, and 11) indicate that the only quantity that converges is pressure. To explain this behavior, it is helpful to recall Eqs. (20) and (39). Both equations are used at different stages of the procedure to evaluate the contravariant velocity components needed at the control volume faces. Equation (39) is used in the pressure equation; therefore the contravariant velocities based on the pressure field always satisfy continuity as long as these contravariant velocities are calculated from Eq. (39). The G values in this equation are obtained by linear interpolation from the nodal values, which are obtained from the momentum equations. On the other hand, Eq. (20) is used after solving the pressure-correction equation to find G_1 and G_2 at the interfaces.

From the above description, different equations are used at two different stages to find the same contravariant velocity components. Further, in view of the correction terms the discretized continuity equation for the pressure-correction equation is different

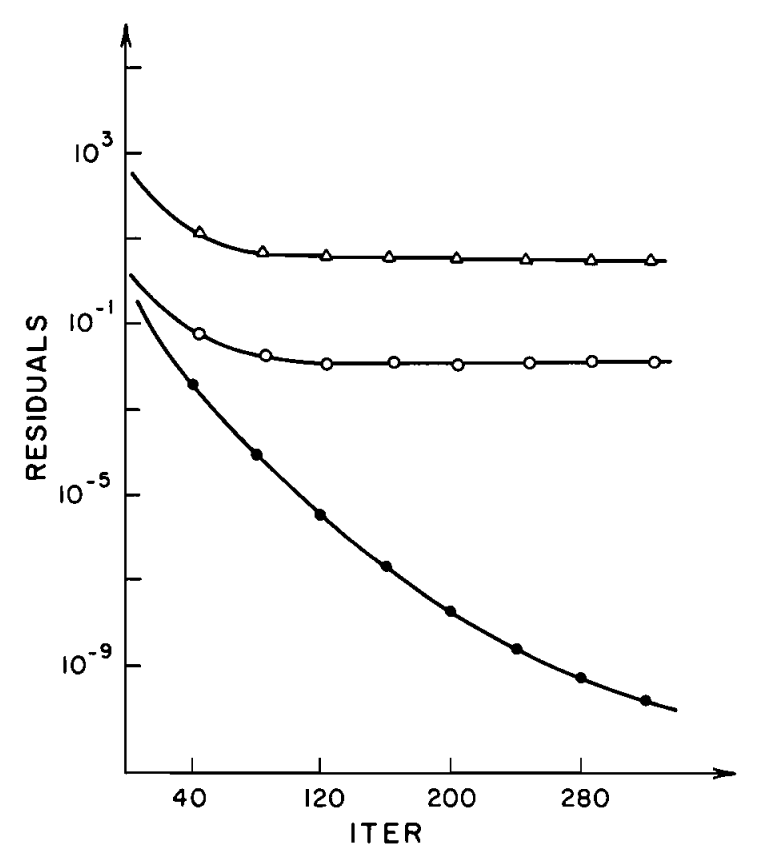


Fig. 11 Maximum residuals of conservation equations for recirculating flow in a sudden expansion obtained with a 14×14 orthogonal mesh and SIMPLER (variable density flow). See Fig. 6 for explanation of symbols.

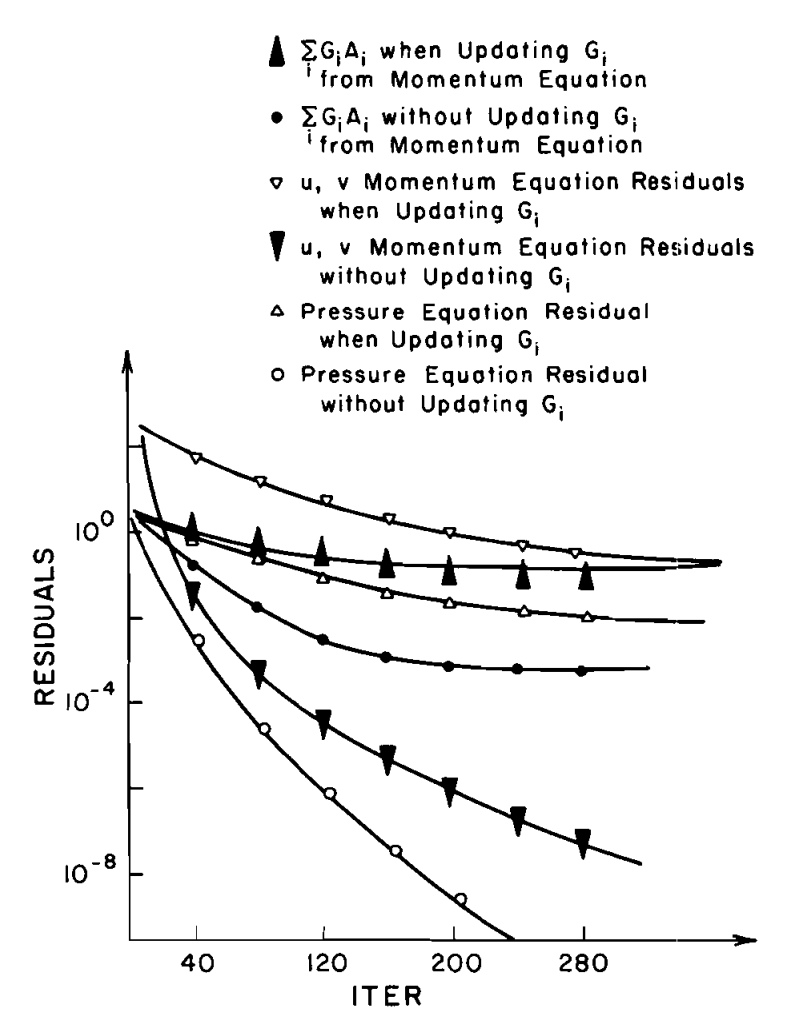


Fig. 12 Maximum residuals of conservation equations for recirculating flow in a sudden expansion obtained with a 14×14 orthogonal mesh and SIMPLEM (variable density flow).

from the discretized continuity equation for the pressure. These discrepancies cause the nonconservative behavior, and as a consequence the converged velocity field from the momentum equation is not identical to the velocity field updated from the pressure-correction equation.

What is learned from this discussion is that, for all quantities to converge, only one of the two discretized continuity equations should be used. This means that one of either Eq. (20) or Eq. (39) should be used to update the contravariant velocity components at the interfaces. One of them [Eq. (20)] is used in SIMPLE (after the p' equation), and the convergence problem arises because of the correction terms that are required to suppress oscillations. SIMPLEM uses the pressure equation without the correction terms but in such a way as to suppress oscillation. A simple idea is found to be effective in accomplishing this objective. This idea is to solve the pressure equation only and to update the

contravariant velocity components needed at the control volume faces by using a centered $1\delta - \xi$ or $1\delta - \eta$ pressure difference scheme in the same equation for the contravariant velocities that is used to derive the pressure equation [Eqs. (39) and (40)]. Therefore any oscillation that arises can be felt, and immediately suppressed, by the interface contravariant velocities, which are always used in calculating the coefficients of the momentum equation. With the new treatment, the only connection between the contravariant and the cartesian velocity components are the G values that are calculated from u and v. A $2\delta - \xi$ or $2\delta - \eta$ difference scheme for the pressure gradients and the G_1 and G_2 values updated in step 5 of the SIMPLEM algorithm by means of a 1δ - scheme for ∇p are used to calculate the coefficients of the momentum equation. The corresponding G_1 and G_2 values in the SIMPLE and SIMPLER algorithms are those that are updated by means of a 1δ- scheme for $\nabla p'$ after the solution of the pressure-correction equation. Therefore, using pressure gradients that are based on a 1δ - ξ or 1δ - η difference scheme for the G values in Eqs. (39) and (40) to obtain (or to update) the contravariant velocity components can be seen as a correction procedure similar to the one used by Rhie and Chow [6] but without the introduction of any extra terms. The additional work done is in the recalculation of the coefficients of the momentum equation after updating the interface velocities to make sure that the velocities used in the coefficients and the pressure field satisfy the same continuity equation. The work involved in this step is actually comparable to calculating the correction terms in SIMPLE and to solving the pressure-correction equation in SIM-PLER. The difference in computer time between SIMPLE and SIMPLEM is about 8%

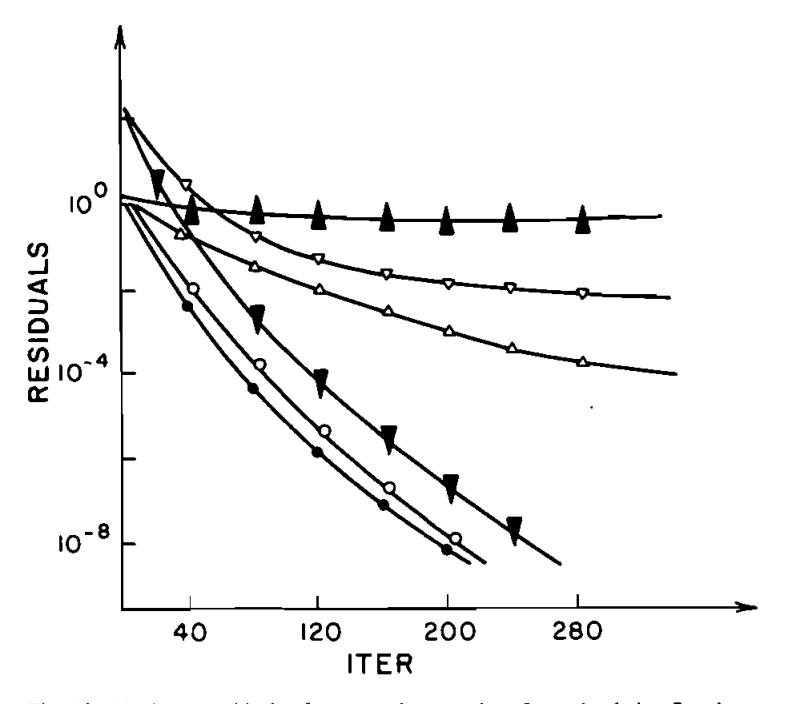


Fig. 13 Maximum residuals of conservation equations for recirculating flow in a sudden expansion obtained with a 14×14 orthogonal mesh and SIMPLEM (constant density flow). See Fig. 12 for explanation of symbols.

(SIMPLEM needs more time). The solutions obtained with this practice show no sign of oscillation.

The results shown in Figs. 8, 9, 12, and 13 indicate the advantages of this treatment, by which the residuals of u, v, and p are always driven to zero. From these figures it is clear that the contravariant components should always be based on continuity (i.e., the pressure equation), and any attempt to update these components from Eq. (7) after solving the momentum equations (step 6 in the SIMPLEM algorithm) creates the same problem noticed in SIMPLER.

If the grid is orthogonal the terms due to nonorthogonality in Eq. (39) cancel, so that there is no need to find the cross-derivatives. For nonorthogonal situations, however, interpolation is needed for these derivatives. This explains the slow convergence of the maximum imbalance of mass shown in Fig. 9. Convergence in this case is to the order of the interpolation, even though the conservation for such cases is at least two orders of magnitude better than the values obtained by SIMPLE and SIMPLER.

The residuals for the case of constant density flow are shown in Fig. 13. In this situation, the convergence behavior is better compared to variable density flow (Fig. 12). It is speculated that for variable density flows the conservation of mass will improve if (ρG) at the interface is directly interpolated instead of interpolating ρ and G separately, as is done here.

CONCLUSIONS

A new algorithm for the solution of two-dimensional elliptic flows in curvilinear coordinates by means of an equal-order pressure-velocity coupling scheme has been presented. This algorithm, called SIMPLEM, is shown to be superior to SIMPLE and SIMPLER algorithms in nonstaggered curvilinear meshes. Oscillation was totally suppressed by a simple yet effective scheme.

REFERENCES

- F. H. Harlow and J. E. Welch, Numerical Calculation of Time-Dependent Viscous Incompressible Flow of Fluid with Free Surface, Phys. Fluids, vol. 8, p. 2182, 1965.
- S. V. Patankar and D. B. Spalding, A Calculation Procedure for Heat, Mass and Momentum Transfer in Three-Dimensional Parabolic Flows, Int. J. Heat Mass Transfer, vol. 15, p. 1787, 1972.
- S. Abdallah, Numerical Solutions for the Pressure Poisson Equation with Neumann Boundary Conditions using a Non-staggered Grid, J. Comp. Physics, vol. 70, p. 187, 1987.
- 4. F. H. Hsu, A Curvilinear-Coordinate Method for Momentum, Heat and Mass Transfer in Domains of Irregular Geometry, Ph.D. thesis, University of Minnesota, Minneapolis, 1981.
- 5. M. Reggio and R. Camarero, Numerical Solution Procedure for Viscous Incompressible Flows, *Numer. Heat Transfer*, vol. 10, p. 131, 1986.
- 6. C. M. Rhie and W. L. Chow, Numerical Study of the Turbulent Flow Past an Airfoil with Trailing Edge Separation, AIAA J., vol. 21, p. 1525, 1983.
- 7. G. E. Schneider, G. D. Raithby, and M. M. Yovanovich, Finite Element Solution Procedures for Solving the Incompressible Navier-Stokes Equations using Equal-Order Variable Interpolation, *Numer. Heat Transfer*, vol. 1, p. 433, 1978.
- 8. R. L. Sani, P. M. Gresho, R. L. Lee, and D. F. Griffiths, The Cause and Cure of the

- Spurious Pressures Generated by Certain FEM Solutions of the Incompressible Navier-Stokes Equations: Part I, Int. J. Numer. Methods Fluids, vol. 1, p. 17, 1981.
- 9. S. V. Patankar, Numerical Heat Transfer and Fluid Flow, McGraw-Hill, New York, 1980.
- 10. O. R. Burggraf, Analytical and Numerical Studies of the Structure of Steady Separated Flows, J. Fluid Mech., vol. 24, p. 113, 1966.
- 11. D. S. Jang, R. Jetli, and S. Acharya, Comparison of the PISO, SIMPLER, and SIMPLEC Algorithms for the Treatment of Pressure Velocity Coupling in Steady Flow Problems, *Numer. Heat Transfer*, vol. 10, p. 209, 1986.

Received March 11, 1988 Accepted September 9, 1988